

E14-2016-24

E. Nyamdavaa<sup>1,\*</sup>, E. Uyanga<sup>1,2</sup>, G. Sevjidsuren<sup>1</sup>, P. Altantsog<sup>1</sup>

PREPARATION AND CHARACTERIZATION  
OF  $\text{La}_{1-x}\text{Ce}_x\text{CoO}_3$  PEROVSKITE OXIDES  
FOR ENERGY MATERIALS

Submitted to “Surface Investigation. X-Ray, Synchrotron  
and Neutron Techniques”

---

<sup>1</sup>Institute of Physics and Technology, Mongolian Academy of Sciences,  
Ulaanbaatar

<sup>2</sup>Joint Institute for Nuclear Research, Dubna

\*E-mail: nyamdavaae@gmail.com

Нямдаваа Э. и др.

E14-2016-24

Получение и характеристика  $\text{La}_{1-x}\text{Ce}_x\text{CoO}_3$  перовскитовых оксидов для энергетических материалов

Церий, легированный лантано-кобальтоперовскитами ( $\text{La}_{1-x}\text{Ce}_x\text{CoO}_3$  при  $x = 0, 0,2, 0,4$ ), был синтезирован по методу золь-геля (обожженного в течение 5 ч при  $750^\circ\text{C}$ ) и характеризуется с помощью дифракции рентгеновских лучей (XRD), поглощения рентгеновских лучей (XAS), энергодисперсионной рентгеновской спектроскопии (EDS) и анализа удельной поверхности BET. Результаты исследования показали, что легирование церия способствовало структурным преобразованиям  $\text{LaCoO}_3$  из ромбоэдрической в кубическую структуру. Высокая удельная поверхность и малый размер кристаллитов достигаются при  $x = 0,2$ . Результаты XAS подтвердили образование соединения  $\text{La}_{1-x}\text{Ce}_x\text{CoO}_3$ .

Работа выполнена в Лаборатории нейтронной физики им. И. М. Франка ОИЯИ.

Препринт Объединенного института ядерных исследований. Дубна, 2016

Nyamdavaa E. et al.

E14-2016-24

Preparation and Characterization of  $\text{La}_{1-x}\text{Ce}_x\text{CoO}_3$  Perovskite Oxides for Energy Materials

Cerium-doped lanthanum cobaltite perovskites ( $\text{La}_{1-x}\text{Ce}_x\text{CoO}_3$  with  $x = 0, 0,2, 0,4$ ) were prepared by the sol-gel method (calcined for 5 h at  $750^\circ\text{C}$ ) and characterized by X-ray diffraction (XRD), X-ray absorption (XAS), energy-dispersive X-ray spectroscopy (EDS), and BET surface area analysis. The results showed that the cerium doping promoted the structural transformation of  $\text{LaCoO}_3$  from rhombohedral into the cubic structure. High specific surface area and small crystallite size are achieved at  $x = 0,2$ . The XAS results confirmed the formation of compound  $\text{La}_{1-x}\text{Ce}_x\text{CoO}_3$ .

The investigation has been performed at the Frank Laboratory of Neutron Physics, JINR.

Preprint of the Joint Institute for Nuclear Research. Dubna, 2016

## 1. INTRODUCTION

Perovskite-type oxides with general formula  $ABO_3$  may potentially replace noble metal catalysts due to their high activity, thermal stability, and low costs [1]. The catalytic properties of  $ABO_3$  basically depend on the nature of A and B ions. Therefore, the electronic properties and catalytic activity of the perovskite-type oxides can be modified by substitution of other heterovalent ions into the A or B sites [2].

Nanostructured perovskites with a high specific surface area and small crystallite size offer the potential for a substantial increase in the performance of catalyst [3,4]. In this work, nanostructured Ce-doped perovskite-type oxides, with  $x$  ranging from 0 to 0.4, were synthesized by the sol-gel method. The prepared powder samples were characterized by XRD, XAS, EDS, and BET methods. The main objective of this work was to study the effect of Ce doping on the structure, surface and absorption properties of  $La_{1-x}Ce_xCoO_3$ .

## 2. EXPERIMENTAL

**2.1. Synthesis of the Sol-Gel Method.**  $La_{1-x}Ce_xCoO_3$  ( $x = 0, 0.2, 0.4$ ) perovskites were prepared by the sol-gel method [5]. Precursors  $La(NO_3)_3 \cdot 6H_2O$  (Roth, 99.995%),  $CeO_2$  (99.95%), and  $Co(NO_3)_2 \cdot H_2O$  (Roth, 99.995%) in appropriate quantities were dissolved in distilled water. Citric acid was added into the mixture in 10 wt.% excess over the stoichiometric quantity to assure the complexation of metal ions. Water was removed at  $80^\circ C$  until a viscous gel was formed. The gel was dried in a vacuum oven set at  $100^\circ C$ . The precursor was then milled and calcined in air at  $750^\circ C$  for 5 h to obtain the perovskite powders.

**2.2. Characterization Measurement.** XRD data were obtained by using Maxima\_X, XRD-7000 equipment with  $CuK_\alpha$  radiation at room temperature. The structural parameters were determined by Rietveld analysis of the diffraction profiles. XAS measurements for Ce  $L_3$ , La  $L_3$  and Co K-edges were recorded at the beam lines BL17C1 of National Synchrotron Center, Hsinchu, Taiwan. The

data fitting was performed using the software package IFEFFIT. The specific surface areas were obtained by  $N_2$ -physisorption, evaluated using the BET equation, on ASAP 2020. EDS elemental analysis was performed using an INCA system.

### 3. RESULTS AND DISCUSSION

The elemental compositions of the catalyst samples determined by energy dispersive spectroscopy analysis are summarized in Table 1. The EDS analysis shows that the composition is almost the same (within experimental error) as the nominal composition of the samples.

Figure 1 shows the XRD patterns of the  $La_{1-x}Ce_xCoO_3$  ( $x = 0, 0.2$  and  $0.4$ ) samples. Typical perovskite peaks for doped samples are well resolved with sharp and intense single peak in the  $LaCoO_3$  pattern [4]. For  $x = 0$ , the structures were the rhombohedral  $LaCoO_3$ -type (JCPD-ICDD 25-1060); when

**Table 1. Energy-dispersive spectroscopy elemental analysis of samples**

Element	$LaCoO_3$		$La_{1-x}Ce_xCoO_3$ ( $x = 0.2$ )	
	N (wt. %)	M (wt. %)	N (wt. %)	M (wt. %)
La	56.50	51.58	45.15	54.79
Co	23.97	33.29	23.94	20.38
O	19.52	15.13	19.5	19.45
Ce			11.38	5.38

*Note.* N — nominal, M — measured.

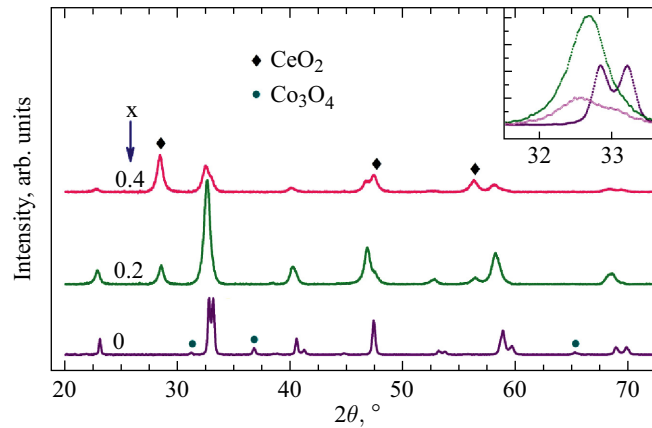


Fig. 1. Experimental powder XRD patterns of  $La_{1-x}Ce_xCoO_3$  samples. With the addition of cerium, mixed phases were expected

$x = 0.2$  and  $0.4$ , the samples exhibited the pattern of cubic  $\text{LaCoO}_3$  (JCPD-ICDD 75-0279). The peaks at  $32.5^\circ$  are found to merge single peak which indicates the transformation of structure from rhombohedral into cubic. This characteristic is a drastic indication for doping influence leading to a space group transformation into cubic lattice symmetry.

The whole patterns shift to lower  $2\theta$  angles for doped samples accordingly with increasing  $x$  as shown in the inset for a typical example for the peak at  $2\theta = 32.5^\circ$ . The decrease of the reflection angle is attributed to larger lattice parameters due to lattice relaxation (Table 2). The dose  $x = 0.4$ , whose peak in the inset is not as sharp as for the case  $x = 0.2$ , might have reached or exceeded the threshold of Ce insertion. More  $\text{CeO}_2$  aggregates (observed at  $2\theta = 28.6^\circ$ ,  $47.4^\circ$ , and  $56.5^\circ$ ) may cause the particles to be disordered or to have smaller coherent length.

Table 2 summarizes the crystallite size, the specific surface area and lattice parameters of all samples. The average crystallite size ( $D$ ) was determined using Debye Scherrer's equation  $D = 0.9\lambda/\beta \cos \theta$ , where  $\lambda$  is the incident X-ray wavelength ( $\lambda_{\text{Cu}} = 1.5443 \text{ \AA}$ ),  $\beta$  is the full width at half maximum (FWHM) of the peak corresponding to maximum intensity, and  $\theta$  represents the diffraction angle of the most intense peak in degrees. The crystallite size of the samples was found to be in the range of 8 to 13 nm, which decreases with increasing Ce content.

**Table 2. XRD and BET analysis results of  $\text{La}_{1-x}\text{Ce}_x\text{CoO}_3$  ( $x = 0, 0.2, 0.4$ ). Lattice parameters enlarged due to lattice relaxation and the crystallite size decreased with the increase of doping concentration**

Samples	Lattice parameter ( $\text{\AA}$ )	Crystallite size (nm)	SSA ( $\text{m}^2 \cdot \text{g}^{-1}$ )
$\text{LaCoO}_3$	$a = b = 5.401, c = 13.312$	13.2	2.18
$\text{La}_{0.8}\text{Ce}_{0.2}\text{CoO}_3$	$a = b = c = 5.379$	12.8	5.68
$\text{La}_{0.6}\text{Ce}_{0.4}\text{CoO}_3$	$a = b = c = 5.384$	8.3	3.32

The specific surface areas (SSA) of samples were relatively low, about  $2\text{--}5 \text{ m}^2 \cdot \text{g}^{-1}$  due to calcinations of perovskites. Calcination at high temperature is necessary to obtain the perovskite-type oxide catalyst, but such treatment often results in a dramatic decrease in the specific surface area. However, the enhancement was not linear with the substitution and SSA was the highest for  $x = 0.2$ .

Figure 2 shows normalized Ce  $L_3$ -edge X-ray absorption near edge structure (XANES) spectra of Ce-doped cobaltites together with the resultant fit. The characteristic double-peaked principal maximum is the signature of the intermediate valence nature [6] arising from excited many body final states with different  $4f$  occupancies. [7]. The Ce  $L_3$  XANES spectra were least-squares fitted with a su-

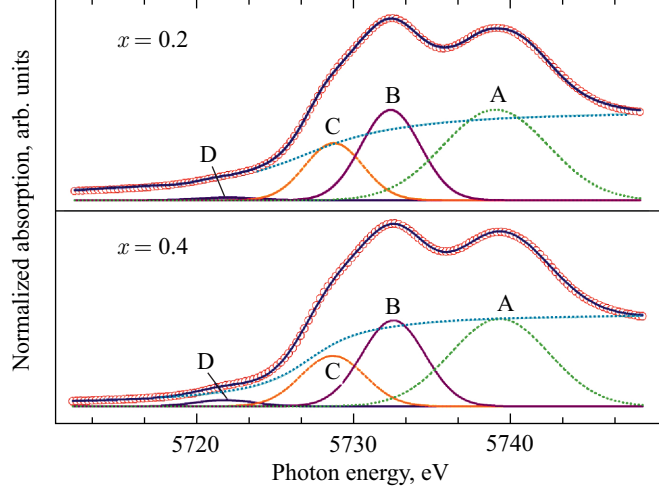


Fig. 2. Ce  $L_3$ XANES spectra of  $\text{La}_{1-x}\text{Ce}_x\text{CoO}_3$  ( $x = 0.2, 0.4$ ) and results of the least-squares-fit analysis (solid line through data open circles)

perposition of various transition components used in some earlier works [8]. Part A is assigned to a core-excited  $\text{Ce}^{4+}$  final state with the configuration  $2p4f^05d^*$ . The peak B probably arises from a  $2p4f^15d^*O$  state of a cerium ion. It highlights the high hybridization of the cerium  $4f$  electrons with the oxygen  $2p$  orbital and demonstrates a two-electron transition. Accordingly, a cerium  $5d^*$  electron excited from its  $2p$  orbital, in an X-ray absorption process, was accompanied by an electron from an O ligand that hybridizes highly with the cerium  $4f$  orbital. The resulting state locates at a slightly higher energy level compared to the peak C which is a fingerprint of a  $\text{Ce}^{3+}$  final state ( $2p4f^15d^*$ ). The pre-edge feature D, which is a small amount being involved in the curve fitting, can be explained by a dipole-forbidden  $2p_{3/2} \rightarrow 4f$  transition.

The Ce  $L_3$ -edge XANESs for the two doped samples look perceptively identical to  $\text{CeO}_2$ . However, comparisons of the energy difference between individual constituents in our samples and between those with the ones of intermetallic compounds and Ce oxide (Table 3) lead to the conclusion of successful cerium incorporation into the lattice of lanthanum cobaltite.

Additionally, the spectral weights of component C resulted from the fitting curves in Fig. 2 were compared with the ones reported by Nachimuthu et al. [9] for  $\text{CeO}_2$ . Notably, the spectral weights of portion C ( $I_C/(I_A + I_B + I_C)$ ) in both doped-compounds are  $\sim 18\%$ , more than three times the value  $\sim 5\%$  reported for  $\text{CeO}_2$  [10]. We hence do not think the  $\text{Ce}^{3+}$  counterpart observed here belongs solely to  $\text{Ce}^{3+}$  impurity of the  $\text{CeO}_2$  aggregates. The effective ionic radius [11] for the twelve-fold coordinated ion is much smaller for  $\text{Ce}^{4+}$  ( $1.14 \text{ \AA}$ ) than that of

**Table 3. Relative position (in eV) of various structures obtained from the second derivatives of the Ce  $L_3$  XANES spectra and spectral weight percentage**

Samples	C	B	A
$\text{La}_{0.8}\text{Ce}_{0.2}\text{CoO}_3$	-10 (18.2%)	-6.7 (29.5%)	0 (52.3%)
$\text{La}_{0.6}\text{Ce}_{0.4}\text{CoO}_3$	-10.6 (18.7%)	-6.8 (31.4%)	0 (49.9%)
$\text{CeO}_2$ [12]	-12.2	-7.3	0
$\text{CeO}_2$ [9]	-10.7	-7.2	0

$\text{Ce}^{3+}$  (1.34 Å), which is comparable to  $\text{La}^{3+}$  (1.36 Å). Therefore, it is likely that some  $\text{Ce}^{3+}$  are present in  $\text{La}_{1-x}\text{Ce}_x\text{CoO}_3$  at La vacant sites to compensate the lattice charge. If we view the picture that the insertions of cerium ions take place at and reduce the number of  $\text{La}^{3+}$  vacancies, the increased lattice parameters found in XRD results are comprehensive.

The experimental La  $L_3$ -edge XANES spectrum, indicated by open circles in Fig. 3, has mainly three structures. The white line (A) with a sharp single peak reflects holes in  $5d$  band while the two post-edge structures B and C denote the contribution of O  $2p$  states hybridizing with La  $5d$  states [12]. We observed the enhanced white lines in the Ce-doped samples and also a slight edge-shift within  $\sim 0.5$  eV (inset of Fig. 3). These data directly prove that La  $5d$  band of the pristine cobaltite is not empty as expected, but instead, partially filled

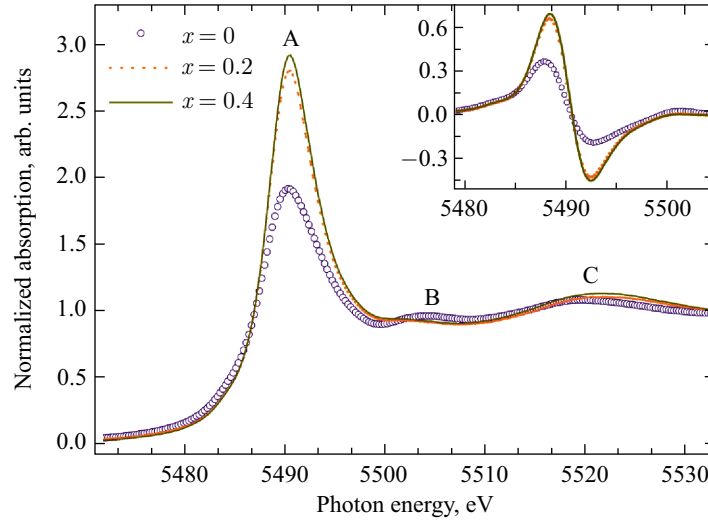


**Fig. 3. Experimental La  $L_3$  XANES spectra and first derivatives of normalized absorption (inset) of  $\text{La}_{1-x}\text{Ce}_x\text{CoO}_3$  with  $x = 0, 0.2,$  and  $0.4$**

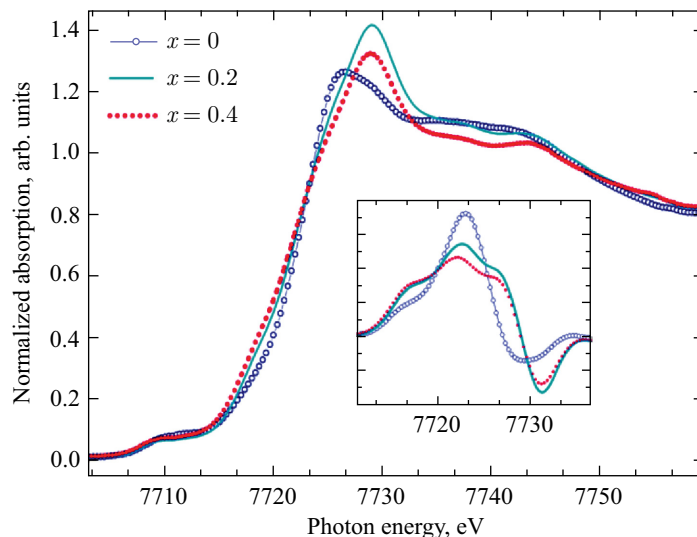


Fig. 4. Experimental Co K-edge XANES spectra and first derivatives (inset) of normalized absorption of  $\text{La}_{1-x}\text{Ce}_x\text{CoO}_3$  with  $x = 0, 0.2,$  and  $0.4$

and becomes less occupied with the effect of Ce doping. The correlation of Ce ionic valence at the Co site was investigated by the measurement of XANES at Co  $K$ -edge. Inset in Fig. 4 presents the normalized XANES spectra at the Co  $K$ -edge, which mainly probe the unoccupied  $4p$  states. The pre-edge peak structure is attributed to  $1s \rightarrow 3d$  quadrupole transitions [13]. Because of no significant change in the pre-edge peak at 7710 eV, it is reasonable to suggest that the coordination number of  $\text{CoO}_6$  octahedron was not affected by Ce doping. The Ce induced blue shift of the Co  $K$ -edge may demonstrate the fact that Co ions gain electrons, and their oxidation states likewise get reduced. Furthermore, the white line was enhanced as the edge slides to lower energies.

## CONCLUSIONS

Nanostructured  $\text{La}_{1-x}\text{Ce}_x\text{CoO}_3$  with a crystallite size of 8–13 nm and a specific surface area of  $2\text{--}5 \text{ m}^2 \cdot \text{g}^{-1}$  were prepared by sol-gel method. The XRD pattern of  $\text{LaCoO}_3$  confirms the sample to be in rhombohedral phase. When cerium is doped, the samples are found to be in cubic phase. An integration of all these results was obtained in the best performance of the sample when  $x = 0.2$ . XAS investigations have proved the actual incorporation of Ce ions, possibly in the forms of  $\text{Ce}^{3+}$ , into the perovskite. The results are in agreement with the increased lattice parameters and the evolution of the symmetry group

into pseudocubic demonstrated by the XRD. These observations are correlated with the enhanced La–O ionic bond and changes in ionic/covalent Co–O bonding properties with increasing Ce-doping concentration.

#### REFERENCES

1. *Mohammad G., Houshang A. // Sensors and Actuators. B. 2011. V. 156. P. 147–155.*
2. *Tejuca G. L. // Chemical Industries. CRC press. Madrid, 1993.*
3. *Williams G., Coles V. S. G. // Mater. Chem. 1998. V. 8. P. 1657–1664.*
4. *Feng J., Liu L., Xu Y. // Ceramics International. 2011. V. 37. P. 1203–1207.*
5. *Khamkar A. K., Bangale V. S. // Appl. Sci. 2014. V. 4. P. 1559–1563.*
6. *Nachimuthu P., Shih C. W., Liu S. R. // J. Solid State Chem. 2000. V. 149. P. 408*
7. *Lee H. C., Oyanagi H., Sekine C. // Phys. Rev. B. 1999. V. 60. P. 13253.*
8. *Dexpert H. et al. // Phys. Rev. B. 1978. V. 36. P. 1750.*
9. *Soldatov V. A. // Phys. Rev. B. 1994. V. 50. P. 5074.*
10. *Shannon D. R. // Acta Crystallogr. A. Sect. 1976. V. 32. P. 751.*
11. *Bridges F. et al. // Phys. Rev. B. 2001. V. 63. P. 214405.*
12. *Pandey K. S., Kumar A. // J. Phys. Condens. Mat. 2006. V. 18. P. 7103–7110.*

Received on March 30, 2016

Редактор *Э. В. Ивашкевич*

Подписано в печать 13.04.2016.

Формат 60 × 90/16. Бумага офсетная. Печать офсетная.

Усл. печ. л. 0,62. Уч.-изд. л. 0,88. Тираж 205 экз. Заказ № 58795.

Издательский отдел Объединенного института ядерных исследований  
141980, г. Дубна, Московская обл., ул. Жолио-Кюри, 6.

E-mail: [publish@jinr.ru](mailto:publish@jinr.ru)

[www.jinr.ru/publish/](http://www.jinr.ru/publish/)